


Characterization of the Onset, Progression, and Reversibility of Morphological Changes in Mouse Lung after Pharmacological Inhibition of Leucine-Rich Kinase 2 Kinase Activity[§]

 Dianne K. Bryce, Chris M. Ware, Janice D. Woodhouse, Paul J. Ciaccio, J. Michael Ellis,¹ Laxminarayan G. Hegde, Sabu Kuruvilla, Matthew L. Maddess, Carrie G. Markgraf, Karin M. Otte, Frederique M. Poulet, Lauren M. Timmins, Matthew E. Kennedy, and Matthew J. Fell

Merck & Co., Inc., Kenilworth, New Jersey; Discovery Neuroscience (D.K.B., C.M.W., C.G.M., F.M.P., L.M.T., M.E.K., M.J.F.), Pharmacology (J.D.W., L.G.H.), Safety Assessment and Laboratory Animal Resources (P.J.C.), Discovery Chemistry (M.L.M.), and PPDM (K.M.O.), Merck & Co., Inc., Boston, Massachusetts; and Safety Assessment and Laboratory Animal Resources, Merck & Co., Inc., West Point, Pennsylvania (S.K., C.G.M., F.M.P.)

Received July 14, 2020; accepted January 20, 2021

ABSTRACT

Gain-of-function mutations in leucine-rich kinase 2 (LRRK2) are associated with increased incidence of Parkinson disease (PD); thus, pharmacological inhibition of LRRK2 kinase activity is postulated as a disease-modifying treatment of PD. Histomorphological changes in lungs of nonhuman primates (NHPs) treated with small-molecule LRRK2 kinase inhibitors have brought the safety of this treatment approach into question. Although it remains unclear how LRRK2 kinase inhibition affects the lung, continued studies in NHPs prove to be both cost- and resource-prohibitive. To develop a tractable alternative animal model platform, we dosed male mice in-diet with the potent, highly selective LRRK2 kinase inhibitor MLI-2 and induced histomorphological changes in lung within 1 week. Oral bolus dosing of MLI-2 at a frequency modeled to provide steady-state exposure equivalent to that achieved with in-diet dosing induced type II pneumocyte vacuolation, suggesting pulmonary changes require sustained LRRK2 kinase inhibition. Treating mice with

MLi-2 in-diet for up to 6 months resulted in type II pneumocyte vacuolation that progressed only modestly over time and was fully reversible after withdrawal of MLI-2. Immunohistochemical analysis of lung revealed a significant increase in prosurfactant protein C staining within type II pneumocytes. In the present study, we demonstrated the kinetics for onset, progression, and rapid reversibility of chronic LRRK2 kinase inhibitor effects on lung histomorphology in rodents and provide further evidence for the derisking of safety and tolerability concerns for chronic LRRK2 kinase inhibition in PD.

SIGNIFICANCE STATEMENT

We have defined a mouse model by which the on-target lung effects of leucine-rich kinase 2 (LRRK2) kinase inhibition can be monitored, whereas previous in vivo testing relied solely on nonhuman primates. Data serve to derisk long-term treatment with LRRK2 kinase inhibitors, as all lung changes were mild and readily reversible.

Introduction

Parkinson disease is a debilitating, progressive movement disorder characterized by the loss of dopaminergic neurons in the substantia nigra pars compacta and is associated with the

accumulation of α -synuclein-containing protein aggregates termed Lewy bodies (Braak and Braak, 2000). Current therapies for PD target the dopaminergic system and have proven beneficial in the treatment of associated motor symptoms but do not impact disease progression (Ellis and Fell, 2017). With the incidence of PD expected to double by the year 2030, estimates indicate that the disease could afflict approximately 10 million patients worldwide (Dorsey et al., 2007), emphasizing the clear need to identify novel targets that can slow or stop disease progression.

One candidate that has emerged as a promising target for disease modification in PD is leucine-rich kinase 2 (LRRK2). The *LRRK2* gene encodes a large multifunctional protein comprised of GTPase and kinase domains flanked by several

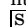
This work received no external funding.

Conflict of interest statement: All authors were or are employees of Merck Sharp & Dohme Corp., a subsidiary of Merck & Co., Inc., Kenilworth, NJ, and shareholders in Merck & Co., Inc., Kenilworth, NJ at the time of their contributions. No author has an actual or perceived conflict of interest with the contents of this article.

¹Current affiliation: Bristol-Myers Squibb, Cambridge, Massachusetts.

The authors would like to inform the reviewers that our colleague Carrie G. Markgraf has died.

<https://doi.org/10.1124/jpet.120.000217>.

 This article has supplemental material available at jpet.aspetjournals.org.

ABBREVIATIONS: BAL, bronchoalveolar lavage; BID, twice daily; C_{min}, minimal plasma blood concentration; GAPDH, glyceraldehyde-3-phosphate dehydrogenase; IHC, immunohistochemistry; LRRK2, leucine-rich kinase 2; NHP, nonhuman primate; PD, Parkinson disease; PK, pharmacokinetic; PO, per os; proSP-C, prosurfactant protein C; QD, every day; pSer935, phospho Serine-935; PPDM, Pharmacodynamics, pharmacokinetics, drug metabolism; SP-D, surfactant protein D.

protein-protein interacting regions (Taylor and Alessi, 2020). Missense mutations in *LRRK2* are the leading cause of monogenic PD, accounting for ~4% of familial cases (Healy et al., 2008), and common variants in the *LRRK2* locus are known risk factors for PD. All pathogenic mutations in *LRRK2* (N1437H, R1441G/C/H, Y1699C, G2019S, and I2020T) increase kinase activity (West et al., 2005), and increased levels of LRRK2 kinase activity have been observed in postmortem brain tissue from patients with idiopathic PD (Wang et al., 2017; Di Maio et al., 2018). Thus, inhibition of LRRK2 kinase activity represents a novel therapeutic strategy for slowing or stopping the progression of PD not only in LRRK2 mutation carriers but also potentially in the more common idiopathic forms of PD.

The ability to safely target LRRK2 kinase activity in the clinic has been called into question after studies conducted in LRRK2-deficient rodents, which identified age-dependent phenotypes in both the kidney and lung. In LRRK2 knockout animals, hyaline droplets and lipofuscin-like brown pigment have been observed in proximal renal tubular epithelium of the kidney, whereas enlarged and vacuolated type II pneumocytes with accumulation of lamellar bodies are seen in the lung (Tong et al., 2010; Herzig et al., 2011; Baptista et al., 2013). Similar results have now been observed after dosing with small-molecule LRRK2 kinase inhibitor compounds. Andersen and colleagues (2018) demonstrated the induction of a kidney phenotype in rats treated with the LRRK2 kinase inhibitor PFE-360. Importantly, these kidney changes were reversible and nonadverse. Efforts to assess the potential of LRRK2 kinase inhibitors to induce a lung phenotype similar to those observed in LRRK2 knockout rodents have relied on studies in nonhuman primates (NHPs) because changes in the lungs of rodents after treatment with LRRK2 kinase inhibitor compounds (Daher et al., 2015; Fuji et al., 2015; Henderson et al., 2015) have not consistently been reported. In NHPs, two LRRK2 kinase inhibitors (GNE-7915 and GNE-0877) have been shown to induce type II pneumocyte vacuolation (Fuji et al., 2015). In a 2-week follow-up study in NHPs, the structurally distinct kinase inhibitors PFE-360 and MLI-2 also induced morphologic changes in the lung, suggesting that the lung phenotype is an on-target effect of LRRK2 kinase inhibition (Scott et al., 2017). LRRK2 kinase inhibition in NHPs did not affect pulmonary function after 15 days of dosing, and the histomorphological changes were reversible after 2 weeks of recovery period (Baptista et al., 2020).

Given that PD is a progressive disorder that will require long-term treatment, understanding the potential for the lung morphologic changes to progress with chronic inhibitor treatment has become critical. Efforts to evaluate this in preclinical studies are challenged by the reliance on NHPs as the responding species, and to date, 28 days is the longest treatment duration studied (Fuji et al., 2015; Baptista et al., 2020). In 2015, we observed the induction of lung morphologic changes in mice after chronic (15 weeks) treatment with MLI-2 using an in-diet dosing paradigm (Fell et al., 2015). Here, we use an alternative animal model paradigm to perform a detailed characterization of the onset, progression, and reversibility of lung morphologic changes by dosing MLI-2 in-diet for up to 6 months. These mouse studies yield reproducible, quantifiable endpoints that are similar to the effects on type II pneumocytes in NHPs and provide a novel model to further investigate the relationship of LRRK2 kinase inhibition with

lung changes that can be applied across novel compounds for treatment of PD.

Materials and Methods

Animals. All studies were carried out in accordance with the policies of the Animal Care and Use Committee of Merck Research Laboratories, Boston, MA, in conjunction with the American Association for the Accreditation of Laboratory Animal Care approved guidelines and the Guide for the Care and Use of Laboratory Animals. C57BL/6J male mice were received from Taconic Farms (Germantown, NY) at 6–8 weeks of age and were singly housed in an environmentally controlled room (temperature $22 \pm 2^\circ\text{C}$ and humidity $>45\%$) on a 12-hour light/dark cycle. All mice were acclimated to the facility for a minimum of 5 days prior to the initiation of study with standard diet (Teklad 2018sx; Envigo, Madison, WI) and water available ad libitum. Each treatment group consisted of four mice, except for the per os (PO) dosing and bronchoalveolar lavage (BAL) collection studies, which used six mice per treatment group.

Test Compound Formulation and Dosing Regimen. MLI-2 and GNE-7915 (Supplemental Fig. 1) were synthesized at Merck Research Laboratories (Boston, MA). For PO dosing, MLI-2 was suspended in a β -cyclodextrin derivative, Captisol (30% solution in water; Ligand Technologies, La Jolla, CA) and dosed at a volume of 10 ml/kg. All other compound treatments were dosed in rodent chow, prepared at Research Diets (New Brunswick, NJ), and formulated to provided doses of 3, 10, 30, 60, or 120 mg/kg per day (MLi-2) or 10, 30, 100, 300 mg/kg per day (GNE-7915) based on an average daily food consumption of 3 g. Mice were first habituated to vehicle diet (D01060501; Research Diets) for 3 days. Chow was then substituted with formulated diet, which was continued for 3–180 days, according to the study design. For some mice, a washout arm was conducted, returning mice to vehicle diet for 1 week. All mice and formulated chow were weighed weekly throughout the study to monitor appropriate weight gain and food consumption.

Terminal Tissue Collection. To preserve lung integrity for histologic assessment, mice were anesthetized using isoflurane to effect, cervical dislocation was applied, and the caudal vena cava was severed to prevent the flow of blood into the base of the lung. One lobe of the lung was first tied off using surgical suture (Covidien Sofsilik, New Haven, CT), then the trachea was cannulated, and the lungs were inflated by injection of 1 to 2 ml 10% formalin. Lungs were then excised; the inflated lungs stored at room temperature in tubes containing additional 10% formalin and sent to Qualtek (Santa Barbara, CA) for embedding in paraffin and sectioning at $5 \mu\text{m}$. The remaining (unfixed) lungs were quick-frozen on a steel plate resting on dry ice and stored at -80°C for analysis of phospho Serine-935 (pSer935) and total LRRK2 levels. For BAL collection, mice were euthanized with an intraperitoneal injection of 0.1 ml Euthasol (Henry Schein, Melville NY). A small incision was made in the trachea, and 1 ml of saline was slowly lavaged through the lung and then recollected into the syringe and placed in collection tubes. BAL fluid was centrifuged at $400g$ for 10 minutes at 4°C , and supernatants were collected and stored at -80°C .

Histopathological Analysis and Image Quantification. Formalin-fixed paraffin-embedded lung sections were either stained with H&E or immunohistochemically stained for prosurfactant protein C (proSP-C) expression in type II pneumocytes. Immunohistochemical staining was carried out on a Ventana Discovery Ultra using the Chromomap detection method. Briefly, lung sections on glass slides were rehydrated, and heat-induced epitope retrieval was performed using a Tris-borate EDTA solution. Slides were then incubated with an anti-proSP-C antibody (AB3786, 1:8000; EMD Millipore) followed by Discovery Omnimap anti-rabbit-horseradish peroxidase (760-4311; Roche Tissue Diagnostics). Signal was visualized using the Discovery Chromomap DAB Kit (Ventana), and slides were counterstained with hematoxylin II (Ventana). The slides were digitized on a Leica XT

scanning microscope (20× magnification), and the area of individual type II pneumocytes in at least 10 randomly selected areas for each lung section was measured using HALO image analysis software version 2.1.1637 (Indica Laboratories, Corrales, NM).

Assessment of Plasma Levels of MLI-2 and GNE-7915. To define pharmacokinetic (PK) properties, mice were dosed PO with 30, 100, or 300 mg/kg MLI-2, and samples were collected at 0.5, 1, 4, 8, and 24 hours postdosing. Plasma samples were assayed for compound levels using liquid chromatography and tandem mass spectrometry analyses as previously described (Fell et al., 2015). For the modeling study, mice ($n = 2$) were orally dosed with 30, 100, and 300 mg/kg of MLI-2. Plasma was sampled at 1 and 8 hours, at 24 hours (1-day C_{max}), at 120 and 128 hours (5 days, C_{max} and C_{min}), and at 144 hours (C_{min}); terminal tissue and plasma samples were collected 12 hours after the last PO dosing to capture target engagement and histopathological changes at MLI-2 plasma exposure levels reflective of C_{min} . Corresponding blood levels were fitted to a one-compartment model using Phoenix 64 (Build 6.3.0.395, WinNonlin version 6.3; Certara, Princeton, NJ). Blood levels of GNE-7915 mice dosed in-diet were detected as described (Fuji et al., 2015).

Western Blot. LRRK2 immunoblotting was run on samples from lung as described previously (Fell et al., 2015). Briefly, 100 μ g of protein lysate was separated using 3%–8% Tris-Acetate gels and then electrotransferred onto polyvinylidene difluoride membranes for 2 hours at 30 V. After blocking with 5% dry milk, blots were probed overnight at 4°C with either anti-pSer935 LRRK2 antibody (1:1000 v/v, ab133450; Abcam, Cambridge, MA), anti-LRRK2 [MJFF2] antibody (1:500 v/v, ab133474; Abcam), or mouse anti-glyceraldehyde-3-phosphate dehydrogenase (GAPDH) (1:20,000 v/v, G8795; Sigma, St. Louis, MO). Membranes were washed with Tris-buffered saline plus Tween-20 three times for 10 minutes and then incubated for 1 hour at room temperature with secondary antibody [donkey anti-rabbit IgG horseradish peroxidase (1:2000; ThermoFisher), goat anti-mouse IgG IRDye 800CW (1:15,000; Li-Cor), or goat anti-mouse IgG IRDye 680RD (1:10,000; Li-Cor)]. After three additional washes with Tris-buffered saline plus Tween-20, blots were developed using SuperSignal enhanced chemiluminescence horseradish peroxidase substrate (ThermoFisher) and imaged on an Odyssey FC system. Image Studio (version 2.0) was used to quantify individual band intensity. The ratio of pSer935 LRRK2 to total LRRK2 protein levels was derived for each sample and expressed as a percentage of within-gel vehicle control lanes. When analyzing samples to assess changes in total LRRK2 protein levels, GAPDH was used as an internal reference protein.

Quantification of Surfactant Protein D Levels in BAL Fluid. For collected BAL fluid, samples were assayed using an ELISA kit specific for mouse surfactant protein D (SP-D) (Quantikine MFSPD0; R&D Systems Inc., Minneapolis, MN) according to insert directions using a 1:500 dilution of BAL fluid.

Statistical Analysis. Data were analyzed using one-way ANOVA with Dunnett's post hoc test comparing treatment groups to vehicle controls (version 7.02; GraphPad Prism Software, Inc.). For studies comparing multiple dosing time points, a two-way ANOVA was used with Dunnett's multiple comparison test for post hoc analysis; level of significance was set to 0.05. Data were represented as mean \pm S.E.M., and the level of significant differences between means was depicted using *** $P < 0.001$, ** $P < 0.01$, and * $P < 0.05$.

Results

Effects of MLI-2 on Phosphorylation of Ser935 LRRK2 in Mouse Lung and Early Detection of Lung Histomorphological Changes after 7 Days of In-Diet Dosing. To define the PK and pharmacodynamic relationship of MLI-2 in C57BL/6J mice and to probe for early indications of pulmonary changes, we first treated mice in-diet for 7 days with a range of doses of MLI-2 (3, 10, 30, 60, or

120 mg/kg per day). Consistent with previous findings, MLI-2 was well tolerated and resulted in normal body weight gains for all groups (Supplemental Fig. 1A). MLI-2 administration resulted in a dose-dependent reduction in the phosphorylation of LRRK2 Ser935 in lung at doses of 30, 60, and 120 mg/kg per day [$F(5,18) = 39.3$; $P < 0.0001$, and no significant decreases in total LRRK2 protein levels were detected (Supplemental Fig. 1C)].

Histopathological assessment of H&E-stained sections revealed minimal enlargement of randomly scattered alveolar epithelial cells having features consistent with type II pneumocytes in the lungs of mice treated with doses of 60 and 120 mg/kg per day for 7 days (Fig. 2A). As compared with vehicle-treated mice, an increase in both size and number of clear round vacuoles induced distension of the cytoplasm that resulted in an increased prominence of many of the type II pneumocytes. Because type II pneumocytes are the primary source of lung surfactant that is released from vesicles and this is required to maintain tissue compliance, we assessed tissue sections for the surfactant-associated protein proSP-C. Immunohistochemical analysis revealed proSP-C immunoreactivity was localized exclusively to type II pneumocytes and appeared elevated in proportion to the increase in intracellular vesicles observed by H&E (Fig. 2B). No changes in lung (H&E or proSP-C staining) were observed at the 3, 10, and 30 mg/kg per day doses, whereas significant increases were seen in both 60- and 120-mg/kg per day doses (Table 1). Relating free unbound plasma concentrations of MLI-2 to peripheral target engagement, we derived the pSer935 LRRK2 IC_{50} in lung to be 1.3 nM, and thus morphologic changes are observed in lung only when plasma levels are sustained and exceed the lung pSer935 LRRK2 $IC_{50} \geq 3$ -fold.

Modeling Exposure Using PO Dosing: Effects of MLI-2 on Lung Target Engagement and Morphologic Changes after 7 Days of PO Dosing (150 mg/kg Twice Daily). Several studies have described a lack of LRRK2-induced morphologic changes in rodent lung after oral dosing with LRRK2 kinase inhibitor compounds (Fuji et al., 2015; Henderson et al., 2015; Andersen et al., 2018). MLI-2-dosed QD for 30 days at 30 mg/kg PO (the IC_{90} for pSer935 LRRK2 inhibition at 1 hour in lung) was without effect in C57BL/6J lung (internal unpublished data); however, 30 mg/kg per day of MLI-2 delivered in-diet was shown to induce morphologic changes in lung of Mitopark mice (Fell et al., 2015). Given rodent lung alterations have only ever been noted after in-diet dosing, we hypothesized that maintenance of a minimal threshold of LRRK2 kinase inhibition is necessary to provoke the enlargement of type II pneumocytes. A comparison of time versus exposure profiles of 30- and 60-mg/kg per day MLI-2 dosed in-diet with a bolus oral dose of 30 mg/kg over a 24-hour period (Fig. 2A) demonstrated that in-diet dosing provided sustained drug exposure in plasma, with minimal peak-to-trough variation relative to bolus delivery. Pharmacokinetic modeling was performed to determine an appropriate dose in mouse to attain steady-state C_{min} levels comparable with those observed with 60 mg/kg per day of in-diet dosing, the minimal dose of MLI-2 that induced the enlargement of type II pneumocytes. The predicted oral dose to yield blood C_{min} at a steady-state level of 2.6 μ M (or 19.8 nM free plasma concentration) was 150 mg/kg BID (Fig. 2B). Accordingly, one group of mice was dosed orally BID with 150 mg/kg MLI-2 for 7 days; vehicle and parallel 60-mg/kg per day MLI-2 in-diet

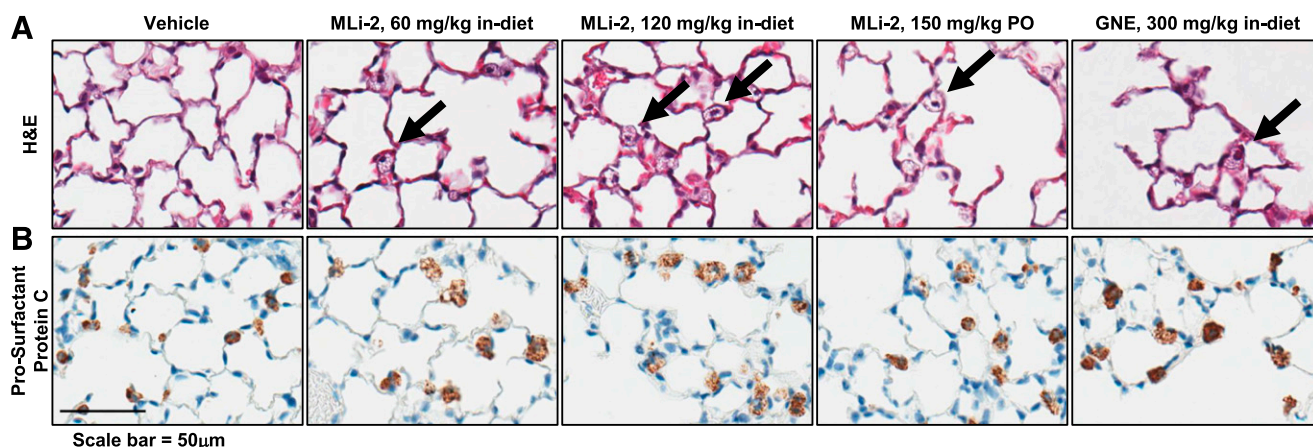


Fig. 1. LRRK2 kinase inhibitors MLI-2 and GNE-7915 induce histomorphological changes in mouse lung. (A) H&E-stained sections revealed changes in lung morphology after 1 week of LRRK2 kinase inhibitor treatment. Arrows indicate slight enlargement of randomly scattered alveolar epithelial cells consistent with type II pneumocytes. (B) Immunohistochemical analysis of lung sections shows that enlarged vessels stain positive for proSP-C.

control groups were also dosed. No tolerability issues were noted in any of the treatment groups. Frequent plasma sampling from the PO-dosed mice confirmed that the model adequately predicted exposures, and the minimal exposure levels observed were always maintained above the lower threshold of 19.8 nM free plasma MLI-2 (Fig. 2B).

As depicted in Fig. 2C, both PO (150 mg/kg BID) and in-diet (60 mg/kg per day) treatments resulted in the significant inhibition of pSer935 LRRK2 in lung [$F(2,11) = 602.2$; $P < 0.0001$]. No significant changes were detected in total LRRK2 protein levels; values were comparable with those obtained for control mice in lung [$F(2,11) = 0.83$; N.S.].

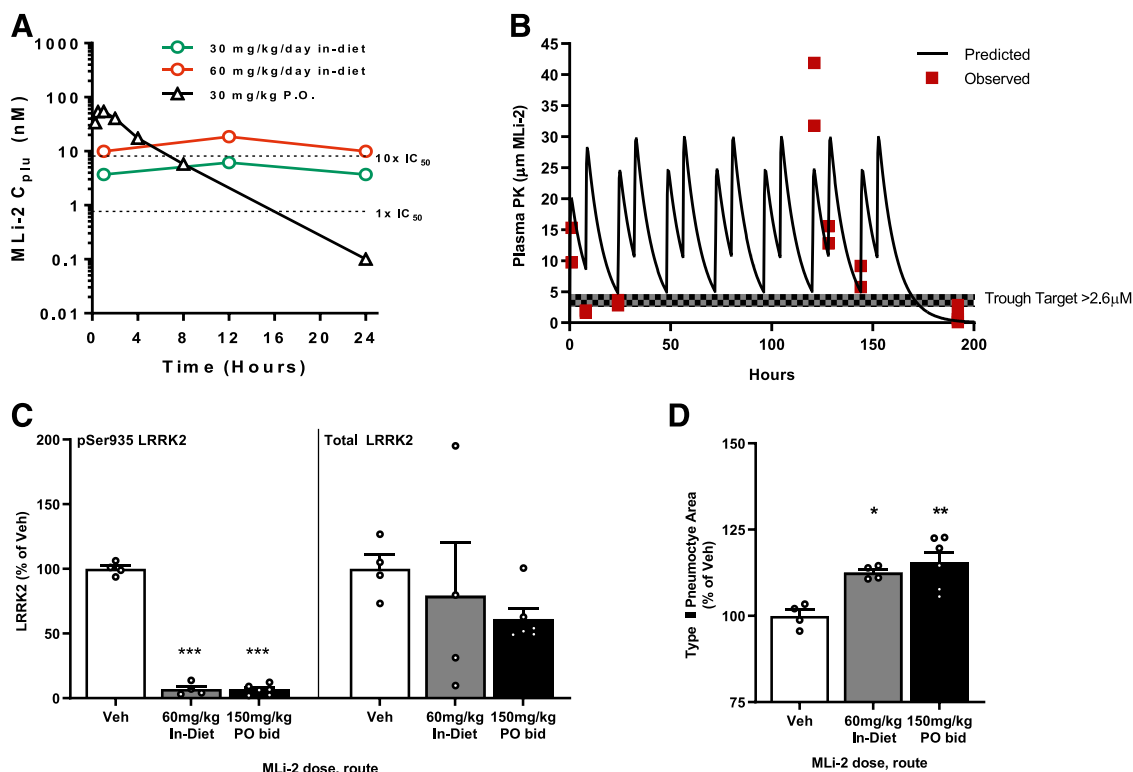


Fig. 2. Pharmacokinetic modeling to predict equivalent MLI-2 PO dosing regimen to recapitulate PD and lung results with 60 mg/kg per day in-diet. (A) Unbound concentrations of MLI-2 after acute or chronic dosing. Mice were treated PO QD for 1 week (triangles) or in-diet with either 30 mg/kg per day (green circles) or 60 mg/kg per day (red circles), and plasma samples were collected at multiple timepoints. Formation of enlarged lung inclusions only manifests when plasma levels were sustained at $\geq 10 \times$ the IC_{50} for MLI-2. (B) Prediction of MLI-2 plasma concentrations over time after PO dosing of MLI-2 BID. Red squares indicate actual plasma concentrations from test mice, and the hatched line represents the minimal trough target exposure predicted to provoke the lung phenotype. (C) Analysis of target engagement expressed as a ratio of pSer935 LRRK2/total LRRK2 or total LRRK2 (normalized to GAPDH) in lung. Mice dosed BID with 150 mg/kg MLI-2 showed robust inhibition of pSer935 equivalent to that seen after 60-mg/kg per day in-diet treatment. Total LRRK2 levels were not significantly changed in either tissue. (D) Quantification of proSP-C-stained areas of lung using HALO image analysis. Both PO and in-diet treatment groups showed significant enlargement of type II pneumocytes. $N = 4-6$ per group. C_{plu} , concentration in plasma, unbound; Veh, vehicle.

TABLE 1

PK and lung data from mice treated for 7 days in-diet with an LRRK2 inhibitor

LRRK2 Compound	Dose	Plasma	TE _{lung} %INH	-Fold over TE _{lung} IC ₅₀	Histopath	Surfactant proSP-C %VEH
	<i>mg/kg per day</i>	<i>u, nM</i>			<i>score per mouse</i>	
MLi-2	3	0.14	0	~	----	~
	10	0.59	26	~	----	~
	30	3.37	89	2.6	----	103
	60	7.50	93	5.8	++++	113
GNE-7915	120	26.2	95	20.3	++++	121
	30	14.5	47	1.2	----	102
	100	21.6	81	1.8	----	104
	300	28.2	89	2.4	+----	111

INH, inhibition; TE, target engagement; u, unbound conc.; VEH, vehicle; +, positive lung finding; - negative lung finding.

Histopathological analysis of the H&E-stained sections revealed that 150 mg/kg MLI-2 PO BID was associated with enlargement of type II pneumocytes in all mice after 7 days of treatment; also noted was an increase in the number and size of vacuoles as compared with vehicle-treated mice (Fig. 1A). One-way ANOVA analysis of IHC staining for proSP-C (Fig. 1B) showed a significant increase in both PO and in-diet dosed groups (Fig. 2D); Dunnett's post hoc analysis resulted in $P < 0.05$ for in-diet treatment and $P < 0.01$ for PO-dosed mice.

Effects of a Structurally Distinct LRRK2 Kinase Inhibitor (GNE-7915) on Biochemical and Immunohistochemical Endpoints in Mouse Lung after 7 Days of In-Diet Dosing. We next assessed whether morphologic changes in lungs of mice could be induced using a structurally distinct LRRK2 kinase inhibitor. GNE-7915 is a small-molecule LRRK2 kinase inhibitor that demonstrates potency, selectivity, and brain penetrability (Fuji et al., 2015). Whereas GNE-7915 was shown to induce lung effects after 7 days of treatment in NHPs at doses ≥ 25 mg/kg per day, studies conducted in mice (up to 300 mg/kg PO BID for 15 days) and rats (up to 100 mg/kg QD for 7 days) did not result in microscopic changes in lung. Here we proposed that using formulated chow to dose GNE-7915 in-diet would achieve sustained plasma levels without incurring tolerability issues. Mice received 10, 30, 100, or 300 mg/kg per day of GNE-7915 in-diet for 7 days. After a brief drop in food intake during days 1–3 of transition to formulated diet, all mice returned to normal body weight by day 7 (Supplemental Fig. 1B). To measure both early and terminal compound exposure, plasma levels were assayed after 3 or 7 days of in-diet dosing. Free plasma exposures of GNE-7915 were stable across days and ranged from 10 to 28 nM (Table 1). Analysis of Western blot images (Fig. 3A) showed GNE-7915 significantly inhibited pSer935 LRRK2 in a dose-dependent manner in lung [$F(4,14) = 28.3$; $P < 0.0001$] with no significant reduction in total protein levels [$F(4,14) = 0.83$, N.S.] (Fig. 3B). Plotting the PK versus PD response (unbound free plasma levels vs. tissue pSer935-LRRK2) yielded the GNE-7915 IC₅₀ to be 12.8 nM in lung. Thus, peripheral exposure to GNE-7915 reached 2.5-fold over the lung IC₅₀ at the maximum tested dose of GNE-7915 (Fig. 3C). Analysis of H&E-stained sections reported one of four treated mice at the highest dose of GNE-7915 (300 mg/kg per day) demonstrated increased vacuolation of type II pneumocytes (Fig. 1A; Table 1). The positive control MLI-2 (120 mg/kg per day) showed increased vacuolation typical of this dose, whereas vehicle and other doses of GNE-7915 were without notable lung histology findings. Post hoc analysis of

proSP-C IHC staining (Fig. 1B) indicated significant increases above vehicle only at 300 mg/kg per day GNE-7915 [$F(4,15) = 6.9$; $P < 0.001$]; Dunnett's test at 300 mg/kg per day $P < 0.01$ (Fig. 3D).

Defining the Time Course and Progression of Lung Effects in Mice Treated with MLI-2 From 3 to 180 Days. To define the earliest detectable changes in lung after initiation of LRRK2 kinase inhibition, to monitor the progression of lung changes after chronic dosing, and to investigate reversibility upon compound withdrawal, mice were dosed in-diet with either 30, 60, or 120 mg/kg per day of MLI-2 for intervals ranging from 3 days to 6 months. One arm of the study included a washout phase in which medicated diet was replaced with vehicle diet for 7 days prior to collection of tissues. MLI-2 was well tolerated with no adverse events being noted in any group for the duration of the study. Inhibition of pSer935 LRRK2 in lung remained relatively constant throughout the treatment phase of the study; a two-way ANOVA revealed a significant effect of dose [$F(2,52) = 662.1$; $P < 0.0001$] and no effect of time on-diet (lung [$F(5,52) = 0.33$; $P = 0.89$]). Total LRRK2 levels in lung tissue were unchanged after chronic treatment with drug with the exception of a transient, significant reduction noted in the 120-mg/kg per day group at the single time point of 7 days [$F(5,52) = 2.78$; $P = 0.027$] in this study.

Microscopic examination of H&E-stained sections of lungs from mice treated with 30 mg/kg per day MLI-2 revealed no morphologic changes at any time point. LRRK2 kinase inhibitor-induced changes in lung were evident after 3 days of dosing at 60 and 120 mg/kg per day and persisted at 7, 14, 28, 90, and 180 days on-diet. There were no degenerative or inflammatory changes at any of the times examined, and the changes neither progressed nor worsened with the extended compound treatment.

Quantification of the area of the type II pneumocytes (Fig. 4) showed dose-related increases in surfactant protein C immunoreactivity (two-way ANOVA drug [$F(3,67) = 94.0$; $P < 0.0001$], time [$F(5,67) = 6.46$; $P < 0.0001$], and drug \times time interaction [$F(15,67) = 2.45$; $P < 0.01$]). Although the 30-mg/kg per day dose was without effect at all times studied, the 120-mg/kg per day dose induced significant increases in proSP-C within 3 days of treatment and remained significantly elevated for 6 months (Dunnett's post-test $P < 0.0001$), consistent with the observation of type II pneumocyte vacuolation upon H&E analysis. Lungs of mice treated with the intermediate dose of MLI-2 (60 mg/kg per day) showed significant increases in proSP-C staining at 7 days and a peak response at 28 days; this effect then regressed at 90 and

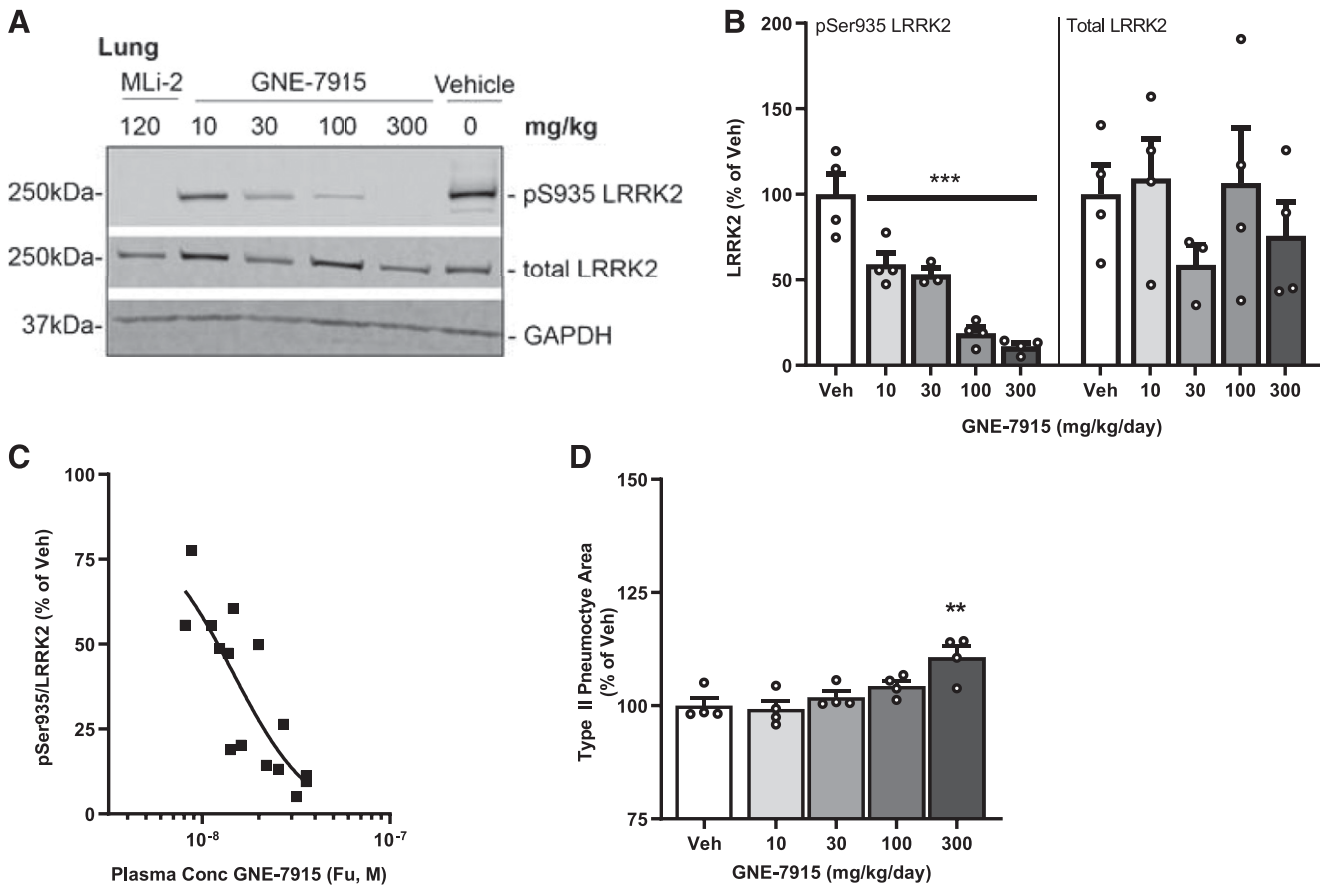


Fig. 3. Biochemical and histologic characterization of lung from mice treated with GNE-7915 in-diet for 7 days. Western blot (A) and quantification (B) of lung samples in which GNE-7915 dose-dependently inhibited pSer935 LRRK2 levels (ratio of pSer935 LRRK2/total LRRK2, expressed as a percentage of the vehicle control group) while having no effect on total LRRK2 protein levels (normalized to GAPDH levels for each band). (C) pSer935 LRRK2 levels in lung vs. unbound concentrations of GNE-7915 (10–300 mg/kg per day) on day 7 of in-diet dosing. (D) GNE-7915 significantly increased area of type II pneumocytes as measured by IHC (proSP-C). Areas were quantified then normalized to the vehicle control group. *N* = 4 per group. Veh, vehicle.

180 days such that by the 6-month time point, proSP-C staining was equivalent to that of vehicle-treated mice (*P* = 0.12 at 3 days; *P* < 0.0001 from 7 to 60 days; *P* = 0.0001 at 90 days; *P* = 0.084 at 180 days).

Histomorphological and Biochemical Changes Are Reversible. To study the reversibility of the observed lung phenotype, lungs and plasma were collected and assayed after a 7-day washout of MLi-2 after 28, 90, and 180 days of dosing in-diet. After 28 dosed days with a 1-week washout, lung pSer935/total LRRK2 reverted to vehicle levels (Supplemental Fig. 2). After 90 days or 180 days of LRRK2 kinase inhibitor treatment with a 7-day washout, the ratio of pSer935/total LRRK2 significantly exceeded control values at 60 mg/kg per day (*P* < 0.01 at both time points) and 120 mg/kg per day (*P* < 0.05 at 90 days). An examination of the Western blot images suggested that this effect was driven by a disproportionate increase in pSer935 LRRK2, although verification of any apparent increase in kinase activity would need to be validated by studying the direct phosphorylation site, Ser1292 LRRK2. Analysis of terminal plasma samples from these mice was consistent with previously observed levels of MLi-2 at the 60- and 120-mg/kg per day doses, and after the washout period, levels of MLi-2 were below the detection limit of the assay (2.5 nM).

H&E-stained lung sections revealed no differences between MLi-2-treated mice (30 mg/kg per day) and vehicle throughout

the study at all time points. With both 60 and 120 mg/kg per day, four of four lungs displayed enlarged type II pneumocytes at all time points (28, 90, and 180 days) except for the 28-day time point at 60-mg/kg per day treatment group in which three of four mice showed histomorphological changes. Complete recovery was observed after the 7day washout period for all chronic dosing groups: 28 days, 3 months, and 6 months dosing

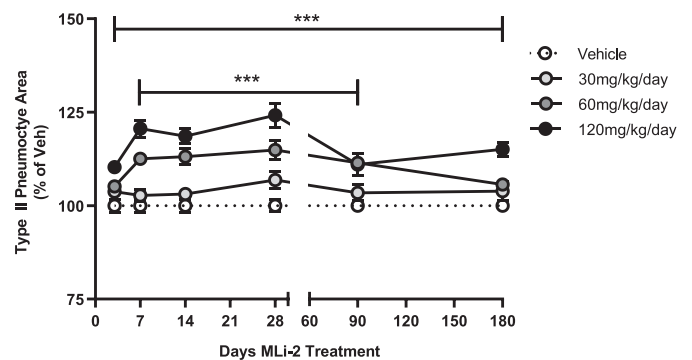


Fig. 4. In-diet dosing with MLi-2 from 3 to 180 days induced modest changes to lung. Within 3 days of dosing and continuing to day 180, 120 mg/kg per day MLi-2 induced significant increases in proSP-C levels as compared with the vehicle control group. Significant increases in the 60-mg/kg per day group are seen after 7 days, peak at day 28, and then revert to normal levels by day 180.

at 60 and 120 mg/kg per day (Fig. 5A depicts 120 mg/kg per day). Quantification of proSP-C (Fig. 5B) depicted a significant increase in type II pneumocyte area after 28 and 90 days with 60 mg/kg per day and at 28, 90, and 180 days at 120 mg/kg per day ($P < 0.01$ when significant). Consistent with the reversal of the enlarged type II pneumocyte morphology observed by histomorphological examination, proSP-C positive area in the lungs of MLI-2-treated groups in the 28, 90, and 180-day washout arms was not different from controls. To determine whether the observed increases in proSP-C could be indicative of decreased surfactant secretion, we measured SP-D levels in BAL fluid from mice that had been dosed in-diet for 28 days and from mice in the washout arm of that study. No changes were detected in SP-D levels in BAL fluid from mice treated with 30, 60, and 120 mg/kg per day (one-way ANOVA, $P = 0.65$) nor after washout of MLI-2 ($P = 0.28$); thus, intracellular accumulation of surfactant proteins caused by LRRK2 kinase inhibition does not appear to result from impaired secretion (Fig. 5C).

Discussion

Inhibition of LRRK2 kinase activity has emerged as an attractive target for slowing the progression of PD in not only LRRK2 mutation carriers but also patients with idiopathic PD (Di Maio et al., 2018). Short-term LRRK2 kinase inhibitor treatment in NHPs leads to increased type II pneumocyte

vacuolation in the lung, raising concerns about the ability to safely inhibit LRRK2 kinase activity in the clinic (Fuji et al., 2015). Here we successfully induced morphologic changes in mouse lung after LRRK2 kinase inhibitor treatment and provided further evidence to allay lung safety concerns. First, we demonstrated that 7-day treatment with the LRRK2 kinase inhibitor MLI-2 via in-diet or PO dosing is sufficient to cause lung changes in mice but only at doses that provide complete and sustained inhibition of LRRK2. Next, dosing MLI-2 for up to 6 months induced changes in lung morphology that occurred rapidly, progressed only slightly, and, after 6 months treatment, stained for prosurfactant protein C at levels indistinguishable from control mice. Third, no detectable changes in SP-D levels were identified in the BAL fluid of mice in which the morphologic change was confirmed. Finally, the morphologic changes induced by MLI-2 treatment were rapidly reversible upon 1 week withdrawal such that, irrespective of MLI-2 treatment duration, normal type II pneumocyte morphology and proSP-C levels were restored. Therefore, lung responses to LRRK2 kinase inhibition reflect rapid, adaptive responses that do not progress and are quickly reversed upon cessation of drug treatment.

In contrast with NHP studies, wherein LRRK2 kinase inhibitor-induced lung changes were noted within 7 days of oral dosing (Fuji et al., 2015; Baptista et al., 2020), visualization of similar pharmacologically induced alterations in

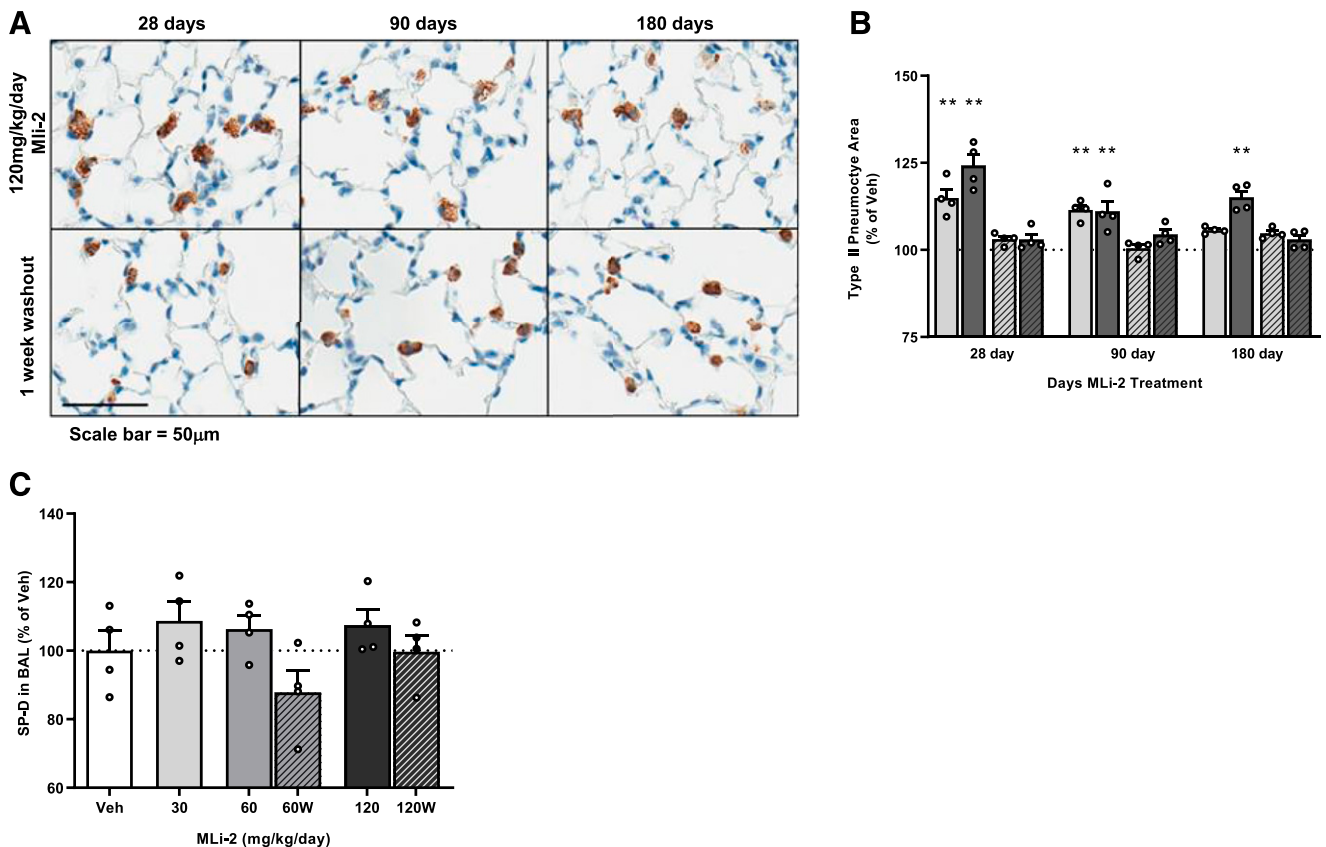


Fig. 5. Biochemical and histomorphological changes to lung after 1–6 months of MLI-2 dosing are reversible with 1-week washout. (A) Observed increases in type II pneumocyte size after 120 mg/kg per day from 28 to 180 days were greatly reduced with 1 week compound washout. (B) Quantification of IHC staining for proSP-C showed significant increases in staining that reverted to baseline after cessation of MLI-2 dosing. (C) No change in surfactant secretion was detected in BAL fluid from mice dosed for 28 days, nor was any effect on compound washout noted. Hatched bars indicate washout of compound. Light bars = 60 mg/kg per day, dark bars = 120 mg/kg per day, and hatched lines indicate washout arm. $N = 4–6$ per group. Veh, vehicle.

rodent lung has proven challenging (Daher et al., 2015; Fuji et al., 2015; Andersen et al., 2018; Kelly et al., 2018). We hypothesized that the transient inhibition of kinase activity achieved with PO dosing in rodents is not sufficient to induce morphologic changes in lung; rather, a sustained, minimal trough level of LRRK2 kinase inhibition is required. This “time on target” hypothesis could be readily tested in mice using in-diet dosing. Indeed, 1 week of in-diet dosing with MLI-2 enabled us to define the relationship between plasma exposure and level of LRRK2 kinase inhibition and morphologic changes in the lung. Importantly, no changes in lung were observed with 30-mg/kg per day dosing, which produced a CC_{min} exposure of $2.8\times$ the LRRK2 pSer935 IC_{50} , yet changes were observed at 60 and 120 mg/kg per day when C_{trough} exposures reached $6\times$ and $20\times$ the LRRK2 pSer935 IC_{50} , respectively. In-diet dosing for 7 days with the structurally distinct GNE-7915 induced a significant increase in proSP-C at 300 mg/kg per day and, combined with the presence of enlarged type II pneumocytes in one of the four mice tested, demonstrated that the lung phenotype was an on-target effect of LRRK2 kinase inhibition. Next, we modeled a PO dosing regimen to maintain MLI-2 plasma exposure above the hypothesized C_{trough} . Not only did we achieve the targeted unbound plasma levels, mimicking that of the 60-mg/kg per day dose in-diet, but we successfully demonstrated LRRK2 kinase inhibitor-induced enlargement of type II pneumocytes after oral gavage dosing along with associated increases in proSP-C. Collectively, these data established that the lung phenotype induced by LRRK2 kinase inhibitors can be observed in mice provided that the plasma exposure is maintained above a minimal threshold. In the case of MLI-2, this threshold is at least $>3\times$ the LRRK2 pSer935 IC_{50} . One limitation of our studies is that only male mice were tested. Although both sexes were equally represented in NHP lung histopathology and toxicology studies with no differences noted (Baptista et al., 2020), additional testing is necessary to extend our findings here across sex.

Having established this lung phenotype in mice, we next sought to leverage this model to perform a detailed kinetic analysis of the onset, progression, and reversibility of the lung morphologic changes. At the lowest in-diet dose (30 mg/kg per day), near-complete inhibition of LRRK2 kinase activity was achieved in the periphery, yet no lung histomorphological changes were detected even after 6 months on-diet. Importantly, at this dose high levels of brain target engagement were observed ($\sim 55\%–85\%$ inhibition of pSer935). These results are consistent with recent observations in NHPs (Baptista et al., 2020), which show that lower doses of MLI-2 and the structurally distinct inhibitor PFE-360 achieved high levels of LRRK2 kinase inhibition in the brain ($>50\%$ inhibition of pSer935) and did not produce the lung phenotype. Although levels of LRRK2 kinase activity required to impact disease progression in patients with PD are yet to be determined, these data collectively suggest that it may be feasible to achieve a margin between high levels of brain LRRK2 kinase inhibition and the induction of the lung phenotype.

Higher doses of MLI-2 (60 and 120 mg/kg per day) produced maximal LRRK2 kinase inhibition and elicited morphologic changes in type II pneumocytes of lungs in as little as 3 days; this change did not progress in size or number of vacuoles in type II pneumocytes over 6 months of sustained LRRK2 kinase inhibition. Moreover, the increase in proSP-C that

accompanied these changes was modest, progressed only slightly from day 3 to 28, and regressed over time such that after 6 months on-diet, proSP-C levels in the 60-mg/kg per day group were indistinguishable from those of controls. Regression in the 60-mg/kg per day group likely suggests that type II pneumocyte trafficking of surfactant can adapt to chronic high levels of LRRK2 kinase inhibition. Importantly, the induction of the lung phenotype was rapidly reversed when inhibition was released such that all morphologic changes completely recovered within 1 week of compound washout. Taken together, these data indicate a dynamic, adaptive response to kinase inhibition and suggest that full recovery can be rapidly achieved upon stopping treatment. Our findings in mice support those of Baptista et al. (2020), who determined the lung phenotype in NHPs to be completely reversible after a 14-day recovery period.

Pulmonary surfactant protein D levels have been assessed as a potential biomarker of lung function in pulmonary disorders, such as chronic obstructive pulmonary disease (Sorensen, 2018). Here, we saw no changes in SP-D levels in BAL fluid regardless of dose or duration of treatment, suggesting that LRRK2 kinase inhibition does not affect surfactant levels in the alveolar space. However, considering the role of LRRK2 in facilitating not only the synthesis and secretion but also the reuptake and reprocessing of surfactant by type II pneumocytes, additional investigation is necessary to fully understand the kinetics of surfactant metabolism with LRRK2 kinase inhibition. Although we have conducted a detailed histomorphological characterization of the lung phenotype, we have not assessed the impact of LRRK2 kinase inhibition on pulmonary function in mice. The functional effects of LRRK2 kinase inhibition have recently been evaluated in NHPs (Baptista et al., 2020) and in humans in an 11-day phase 1b study with DNL-201 with no dose-dependent changes to pulmonary function observed. Finally, loss-of-function variants in LRRK2 are not strongly associated with any adverse phenotypes (Whiffin et al., 2020).

Inhibition of LRRK2 kinase activity results in the destabilization of the LRRK2 protein (Herzig et al., 2011; Zhao et al., 2015; Lobbestael et al., 2016), and it has been suggested that inhibitor-induced reductions in LRRK2 protein levels are critical to the induction of the lung phenotype (Herzig et al., 2011) (Herzig et al., 2011) (Herzig et al., 2011). Here, we demonstrated the emergence of lung effects within 3 days of dosing, yet a decrease in lung total LRRK2 protein was only observed at a single (7-day) time point in one study. Our data not only suggest that inhibitor-induced decreases in protein levels are not likely to be exclusively responsible for the induction of lung histomorphological changes but also confirm previous reports that observed the induction of the lung phenotype in NHPs without attendant alterations in total LRRK2 levels (Fuji et al., 2015; Baptista et al., 2020). Although the underlying molecular mechanism by which inhibition of LRRK2 kinase activity leads to accumulation of surfactant proteins in type II pneumocytes remains unclear, alterations in the endolysosomal pathway may be involved. LRRK2 has been shown to phosphorylate a subset of Rab GTPases (Steger et al., 2016), which play a critical role in regulating vesicular trafficking. Specifically, phosphorylation at Thr-73 on Rab10 blocks its interaction with GDP dissociation inhibitors, leading to the accumulation of membrane-bound, inactive Rab proteins (Eguchi et al., 2018). We propose

that near-complete inhibition of LRRK2 kinase activity may also disrupt the balance of membrane-bound active versus inactive Rab proteins, leading to lysosomal dysfunction and the emergence of the lung phenotype. Studies to further explore the molecular mechanism of the lung morphologic changes in response to LRRK2 kinase inhibitor treatment are currently underway.

Sustained and complete inhibition of LRRK2 kinase activity leads to the rapid induction of a lung phenotype in mice. These lung changes do not progress over 6 months of treatment and are without measurable impact on surfactant protein D secretion. Importantly, this lung phenotype rapidly normalizes upon cessation of compound administration. Although monitoring pulmonary function will be a key component in LRRK2 kinase inhibitor clinical studies, these data, combined with results from the MJFF LRRK2 Safety Initiative in NHPs, suggest that the morphologic changes in type II pneumocytes should not prevent the continued clinical evaluation of LRRK2 kinase inhibitors for PD.

Acknowledgments

The authors thank Cheryl Leyns for her assistance in formatting Western blot images for this manuscript.

Authorship Contributions

Participated in research design: Bryce, Hegde, Otte, Fell.

Conducted experiments: Bryce, Woodhouse, Timmins.

Contributed new reagents or analytic tools: Ellis, Maddess.

Performed data analysis: Bryce, Ware, Ciaccio, Kuruvilla, Markgraf, Otte, Poulet, Timmins.

Wrote or contributed to the writing of the manuscript: Bryce, Ware, Otte, Kennedy, Fell.

References

- Andersen MA, Wegener KM, Larsen S, Badolo L, Smith GP, Jeggo R, Jensen PH, Sotty F, Christensen KV, and Thougard A (2018) PFE-360-induced LRRK2 inhibition induces reversible, non-adverse renal changes in rats. *Toxicology* **395**: 15–22.
- Baptista MA, Dave KD, Frasier MA, Sherer TB, Greeley M, Beck MJ, Varsho JS, Parker GA, Moore C, Churchill MJ, et al. (2013) Loss of leucine-rich repeat kinase 2 (LRRK2) in rats leads to progressive abnormal phenotypes in peripheral organs. *PLoS One* **8**:e80705.
- Baptista MAS, Merchant K, Barrett T, Bhargava S, Bryce DK, Ellis JM, Estrada AA, Fell MJ, Fiske BK, Fuji RN, et al. (2020) LRRK2 inhibitors induce reversible changes in nonhuman primate lungs without measurable pulmonary deficits. *Sci Transl Med* **12**:eaav820.
- Braak H and Braak E (2000) Pathoanatomy of Parkinson's disease. *J Neurol* **247** (Suppl 2):II3–II10.
- Daher JP, Abdelmotilib HA, Hu X, Volpicelli-Daley LA, Moehle MS, Fraser KB, Needle E, Chen Y, Steyn SJ, Galatsis P, et al. (2015) Leucine-rich repeat kinase 2 (LRRK2) pharmacological inhibition abates α -synuclein gene-induced neurodegeneration. *J Biol Chem* **290**:19433–19444.
- Di Maio R, Hoffman EK, Rocha EM, Keeney MT, Sanders LH, De Miranda BR, Zharikov A, Van Laar A, Stepan AF, Lanz TA, et al. (2018) LRRK2 activation in idiopathic Parkinson's disease. *Sci Transl Med* **10**:eaar5429.
- Dorsey ER, Constantinescu R, Thompson JP, Biglan KM, Holloway RG, Kieburtz K, Marshall FJ, Ravina BM, Schifitto G, Siderowf A, et al. (2007) Projected number of

- people with Parkinson disease in the most populous nations, 2005 through 2030. *Neurology* **68**:384–386.
- Eguchi T, Kuwahara T, Sakurai M, Komori T, Fujimoto T, Ito G, Yoshimura SI, Harada A, Fukuda M, Koike M, et al. (2018) LRRK2 and its substrate Rab GTPases are sequentially targeted onto stressed lysosomes and maintain their homeostasis. *Proc Natl Acad Sci USA* **115**:E9115–E9124.
- Ellis JM and Fell MJ (2017) Current approaches to the treatment of Parkinson's Disease. *Bioorg Med Chem Lett* **27**:4247–4255.
- Fell MJ, Mirescu C, Basu K, Cheewatrakoolpong B, DeMong DE, Ellis JM, Hyde LA, Lin Y, Markgraf CG, Mei H, et al. (2015) MLI-2, a potent, selective, and centrally active compound for exploring the therapeutic potential and safety of LRRK2 kinase inhibition. *J Pharmacol Exp Ther* **355**:397–409.
- Fuji RN, Flagella M, Baca M, Baptista MA, Brodbeck J, Chan BK, Fiske BK, Honigberg L, Jubb AM, Katavolos P, et al. (2015) Effect of selective LRRK2 kinase inhibition on nonhuman primate lung. *Sci Transl Med* **7**:273ra15.
- Healy DG, Falchi M, O'Sullivan SS, Bonifati V, Durr A, Bressman S, Brice A, Aasly J, Zabetian CP, Goldwurm S, et al.; International LRRK2 Consortium (2008) Phenotype, genotype, and worldwide genetic penetrance of LRRK2-associated Parkinson's disease: a case-control study. *Lancet Neurol* **7**:583–590.
- Henderson JL, Kormos BL, Hayward MM, Coffman KJ, Jasti J, Kurumbail RG, Wager TT, Verhoest PR, Noell GS, Chen Y, et al. (2015) Discovery and preclinical profiling of 3-[4-(morpholin-4-yl)-7-TH-pyrrolo[2,3-d]pyrimidin-5-yl]benzotriazole (PF-06447475), a highly potent, selective, brain penetrant, and in vivo active LRRK2 kinase inhibitor. *J Med Chem* **58**:419–432.
- Herzig MC, Kolly C, Persohn E, Theil D, Schweizer T, Hafner T, Stemmelen C, Troxler TJ, Schmid P, Danner S, et al. (2011) LRRK2 protein levels are determined by kinase function and are crucial for kidney and lung homeostasis in mice. *Hum Mol Genet* **20**:4209–4223.
- Kelly K, Wang S, Boddu R, Liu Z, Moukha-Chafiq O, Augelli-Szafran C, and West AB (2018) The G2019S mutation in LRRK2 imparts resiliency to kinase inhibition. *Exp Neurol* **309**:1–13.
- Lobbestael E, Civiero L, De Wit T, Taymans JM, Greggio E, and Baekelandt V (2016) Pharmacological LRRK2 kinase inhibition induces LRRK2 protein destabilization and proteasomal degradation. *Sci Rep* **6**:33897.
- Scott JD, DeMong DE, Greshock TJ, Basu K, Dai X, Harris J, Hruza A, Li SW, Lin SI, Liu H, et al. (2017) Discovery of a 3-(4-pyrimidinyl) indazole (MLI-2), an orally available and selective leucine-rich repeat kinase 2 (LRRK2) inhibitor that reduces brain kinase activity. *J Med Chem* **60**:2983–2992.
- Sorensen GL (2018) Surfactant protein D in respiratory and non-respiratory diseases. *Front Med (Lausanne)* **5**:18.
- Steger M, Tonelli F, Ito G, Davies P, Trost M, Vetter M, Wachter S, Lorentzen E, Duddy G, Wilson S, et al. (2016) Phosphoproteomics reveals that Parkinson's disease kinase LRRK2 regulates a subset of Rab GTPases. *eLife* **5**:e12813.
- Taylor M and Alessi DR (2020) Advances in elucidating the function of leucine-rich repeat protein kinase-2 in normal cells and Parkinson's disease. *Curr Opin Cell Biol* **63**:102–113.
- Tong Y, Yamaguchi H, Giaime E, Boyle S, Kopan R, Kelleher RJ III, and Shen J (2010) Loss of leucine-rich repeat kinase 2 causes impairment of protein degradation pathways, accumulation of alpha-synuclein, and apoptotic cell death in aged mice. *Proc Natl Acad Sci USA* **107**:9879–9884.
- Wang S, Liu Z, Ye T, Mabrouk OS, Maltbie T, Aasly J, and West AB (2017) Elevated LRRK2 autophosphorylation in brain-derived and peripheral exosomes in LRRK2 mutation carriers. *Acta Neuropathol Commun* **5**:86.
- West AB, Moore DJ, Biskup S, Bugayenko A, Smith WW, Ross CA, Dawson VL, and Dawson TM (2005) Parkinson's disease-associated mutations in leucine-rich repeat kinase 2 augment kinase activity. *Proc Natl Acad Sci USA* **102**: 16842–16847.
- Whiffin N, Armean IM, Kleinman A, Marshall JL, Minikel EV, Goodrich JK, Quaipe NM, Cole JB, Wang Q, Karczewski KJ, et al.; Genome Aggregation Database Production Team; Genome Aggregation Database Consortium; 23andMe Research Team (2020) The effect of LRRK2 loss-of-function variants in humans. *Nat Med* **26**: 869–877.
- Zhao J, Molitor TP, Langston JW, and Nichols RJ (2015) LRRK2 dephosphorylation increases its ubiquitination. *Biochem J* **469**:107–120.

Address correspondence to: Dianne K. Bryce, Merck & Co., Inc., 33 Ave. Louis Pasteur, Boston, MA 02115. E-mail: Brycedk1@gmail.com; or Dr. Matthew J. Fell, Merck Research Laboratories, Office 8-122, 33 Ave. Louis Pasteur, Boston, MA 02115. E-mail: matthew.fell@merck.com

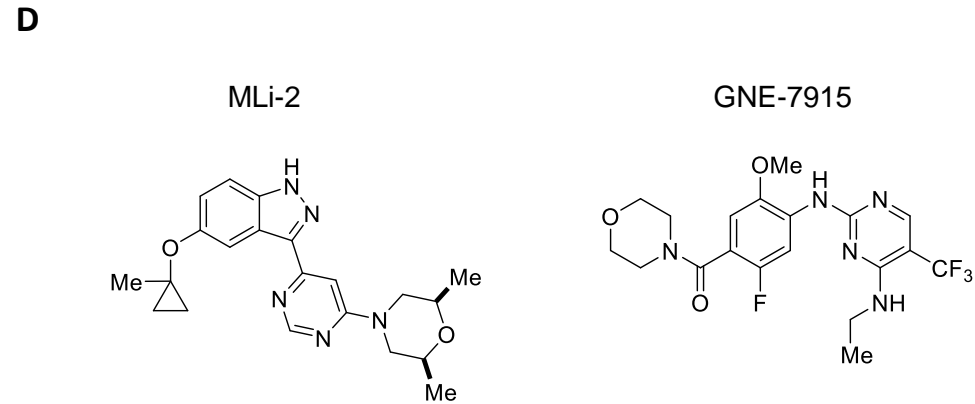
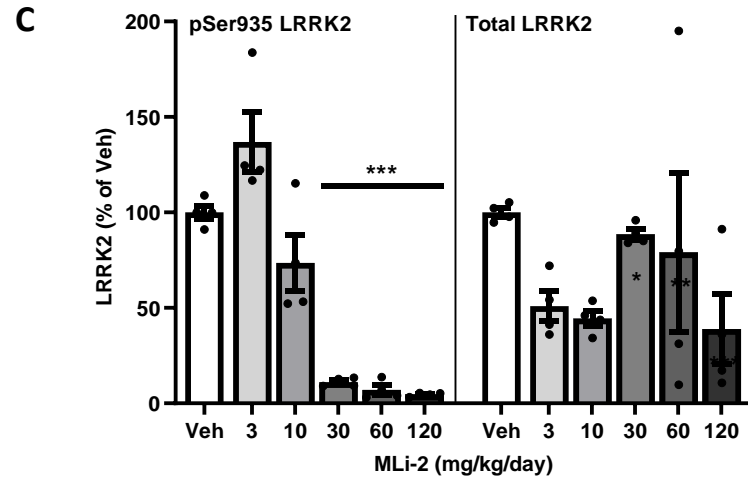
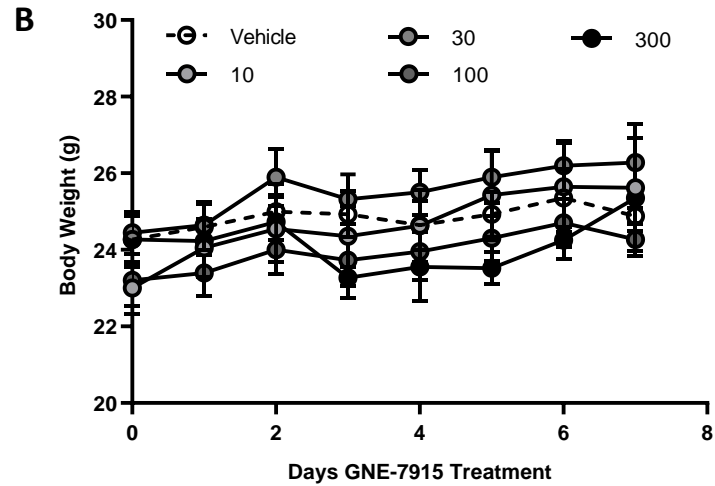
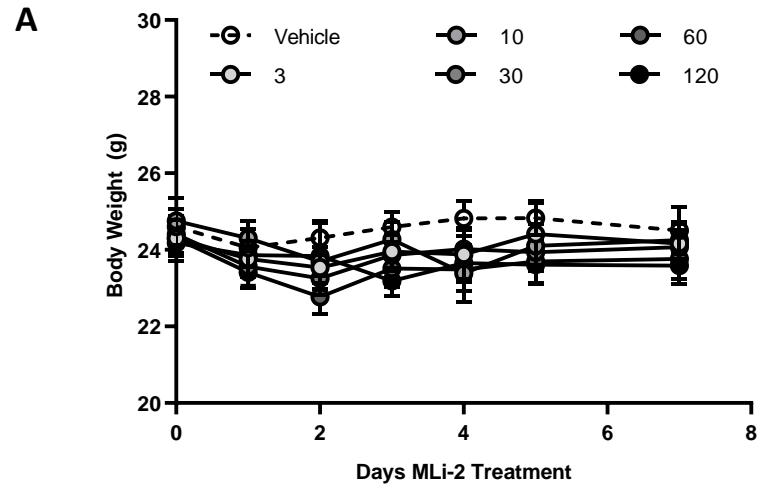
Characterization of the onset, progression, and reversibility of morphological changes in mouse lung following pharmacological inhibition of LRRK2 kinase activity

Dianne K. Bryce, Chris M. Ware, Janice D. Woodhouse, Paul J. Ciaccio, J. Michael Ellis, Laxminarayan G. Hegde, Sabu Kuruvilla, Matthew L. Maddess, Carrie G. Markgraf, Karin M. Otte, Frederique M. Poulet, Lauren M. Timmins, Matthew E. Kennedy, Matthew J. Fell.

Journal of Pharmacology and Experimental Therapeutics

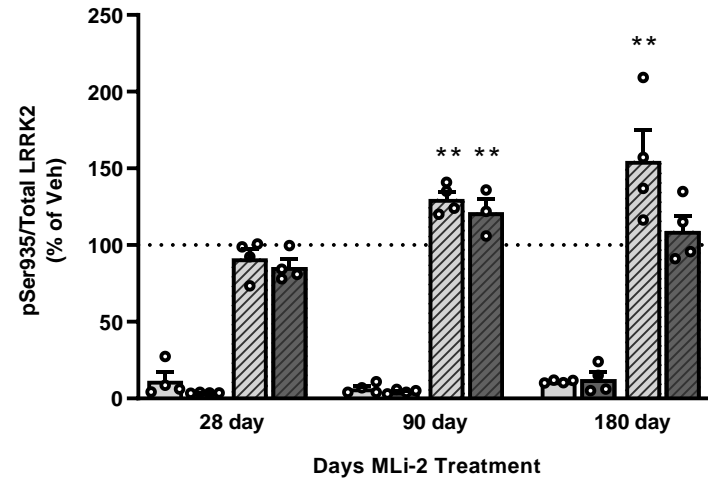
Manuscript number: JPET-AR-2020-000181

Supplemental Fig. 1. BWs \pm SEM of mice dosed in-diet for 7 days with (A) MLi-2 (N=8) or (B) GNE-7915 (N=4) do not differ from BWs of vehicle-treated mice. Numbers indicate dose in mg/kg/day. (C) In lung, pSer935 and total LRRK2 levels were quantified via western blot and expressed as a percentage of the vehicle control groups. N=3-4 per tissue per group.



Supplemental Fig. 2. A) Near-complete inhibition of lung pSer935 LRRK2 persisted with chronic MLI-2 dosing and was released following removal of MLI-2 from chow for 7 days. (B) Western blot showing pSer935 LRRK2, total LRRK2, and GAPDH levels in lung, from 28 to 180 days treatment with MLI-2, and after a 7 day washout. Light bars = 60 mg/kg/day, dark bars = 120 mg/kg/day, hatched lines indicate washout arm.

A



B

